Astron. Astrophys. 330, 953–962 (1998)

ASTRONOMY
AND
ASTROPHYSICS

Towards a consistent model of the Galaxy

II. Derivation of the model

D. Méra[1,3], **G. Chabrier**[1], **and R. Schaeffer**[2]

[1] C.R.A.L. (UMR CNRS 5574), Ecole Normale Supérieure, F-69364 Lyon Cedex 07, France,
[2] Service de Physique Théorique, CEA Saclay, F-91191 Gif-sur-Yvette, France
[3] Physics Department, Whichita State University, 1845 Fairmount, Wichita KS 67260, USA

Received 30 April 1997 / Accepted 24 September 1997

Abstract. We use the calculations derived in a previous paper (Méra, Chabrier and Schaeffer, 1997), based on observational constraints arising from star counts, microlensing experiments and kinematic properties, to determine the amount of dark matter under the form of stellar and sub-stellar objects in the different parts of the Galaxy. This yields the derivation of different mass-models for the Galaxy. In the light of *all* the aforementioned constraints, we discuss two models that correspond to different conclusions about the nature and the location of the Galactic dark matter. In the first model there is a small amount of dark matter in the disk, and a large fraction of the dark matter in the halo is still undetected and likely to be non-baryonic. The second, less conventional model is consistent with entirely, or at least predominantly baryonic dark matter, under the form of brown dwarfs in the disk and white dwarfs in the dark halo. We derive observational predictions for these two models which should be verifiable by near future infrared and microlensing observations.

Key words: stars: low-mass, brown dwarfs – Galaxy: stellar content – Galaxy: halo – cosmology: dark matter

1. Introduction

One of the outstanding problems in astrophysics is the nature of dark matter in the Universe. Over a wide range of scales the dynamics of gravitationally bound systems reveals the presence of a large, dominant amount of dark material. There are in fact two dark matter problems. The "large-scale" dark matter that is the main contributor to Ω is essentially non-baryonic, if $\Omega > 0.1$. And the "galactic" dark matter, whose presence is inferred from the small-scale (velocity dispersion) and large-scale (circular rotation velocity) kinematic properties in galaxies. On the other hand primordial nucleosynthesis, in particular the concordance of the predictions of ^{4}He, ^{3}He, ^{2}H and ^{7}Li abundances bounds Ω_B, with a lower limit $\Omega_B \sim 0.01\,h^{-2}$ (h is the Hubble constant in unit of 100 km.s^{-1} Mpc^{-1}) which exceeds the density of visible baryons (see e.g. Carr, 1994; Copi, Schramm and Turner, 1995). Coincidentally, galactic halos span the range where dark matter could be entirely baryonic, providing a halo radius $R_h \lesssim 50\,h^{-1}$ kpc.

Within the past few years, microlensing observations in the central parts and in the halo of our Galaxy shed new light on the galactic dark matter problem by revealing the presence of dark objects in the Galaxy and thus of "some" baryonic dark matter in the Milky Way. In a previous paper (Méra, Chabrier & Schaeffer, 1997; Paper I) we have examined the different observational constraints arising from star counts at faint magnitudes, kinematic properties and microlensing experiments to derive mass functions in the Galactic disk and halo and to determine as accurately as possible the stellar and substellar contributions to the Galactic mass budget.

In this paper, we examine different mass-models for the Galaxy compatible with these determinations and thus with *all* presently available observational constraints. In Sect. 2, we first discuss the nature of the possible stellar content of the halo. In Sect. 3, we examine what we call the conventional scenario, with a standard massive halo and a substantial fraction of unidentified, most likely *non-baryonic* matter. In Sect. 4, we devote some attention to the maximal disk scenario, whose interest has been renewed in the last years. Sect. 5 is devoted to the derivation of a less conventional model, which determines the limits of an *entirely-baryonic* dark matter model for the Galaxy. Summary and conclusions are outlined in Sect. 6. We propose observational predictions characteristic of these models which should be in reach of near future infrared and microlensing projects.

2. Which objects in the dark halo ?

The first analysis of the Hubble Space Telescope (HST) deep star counts showed that M-dwarfs provide at most $\sim 10-20\%$ of the halo dynamical mass (Bahcall et al., 1994; Santiago, Gilmore & Elson, 1996). A more detailed analysis, consistent with the

observed number of high-velocity subdwarfs in the solar neighborhood (Dahn et al, 1995) places much more stringent limits with a main sequence star contribution to the halo mass smaller than 1% (Méra, Chabrier & Schaeffer, 1996; Graff & Freese, 1996; Chabrier & Méra, 1997a; Méra et al., 1997, Paper I). Therefore M-dwarfs are definitely excluded as a significant halo population and can be responsible for less than 0.1 of the 6 to 8 events[1] observed towards the LMC (see Paper I). This raises a severe problem for the observed microlensing events towards the LMC. The nature of the objects responsible for these events is still under debate, and represents a central issue for any model of the Galaxy.

The optical depth inferred from the LMC observations is $\tau_{\rm obs} = 2.2 \pm 1 \times 10^{-7}$, and the average mass for the lens is $\langle\sqrt{m}\rangle^2 \approx 0.5\,{\rm M}_\odot$ (Alcock et al., 1996b). This mass is determined with a standard, spherically symmetric, halo model (see Paper I Sect. 4.3). The velocity dispersion decreases with oblateness, leading to a lower average mass. Within the range of flattened Evans models (Evans, 1993; 1994), the characteristic mass of lenses remains larger than 0.1 $M_\odot$ (see Paper I Sect. 4.3). Only with a very flattened halo (axis ratio of the order of 1/10), the velocity dispersion is low enough for the average mass to lie under the hydrogen burning limit. Moreover, such a disk-like halo must have a relatively small asymmetric drift, which yields an even lower $\langle 1/v_\perp\rangle^{-1}$ and an average lens mass $\langle\sqrt{m}\rangle^2 \approx 0.08{\rm M}_\odot$. But the spheroid MF normalization at 0.1 $M_\odot$ (Eq. (16) of Paper I) is reasonably well constrained. Chabrier and Méra (1997a) have shown that the local spheroid subdwarfs are not related to the dark matter halo, yielding an even more severe constraint on the dark halo MF, whose maximum normalization is $\sim$ 1% of the spheroid one at 0.1 $M_\odot$. Moreover, the extrapolation of the spheroid MF into the brown dwarf domain down to a minimum mass corresponding to an average mass of 0.08 $M_\odot$ yields a mass density of less than 2% of the dark halo density. Clearly, the substellar part of that MF would have to be a Dirac delta-function at 0.08 $M_\odot$ for the whole observed LMC optical depth to be due to brown dwarfs and these brown dwarfs should be visible in the Hubble Deep Field. In any case a highy flattened halo raises severe problems. Features like the Magellanic Stream, for example, can not be accounted for in such a model. Reasonable values for the halo oblateness are more in the range $q \sim 0.6$ (e.g. Sackett et al., 1994), so that brown dwarfs seem to be definitely excluded as halo dark matter candidates, unless they are strongly inhomogeneously distributed in dark clusters (Kerins, 1997).

The expected number of microlensing events in the LMC itself is:

$$N_{\rm LMC} \approx \frac{\sigma}{25\ {\rm km.s^{-1}}} \sqrt{\frac{h}{250\,pc}}\ \frac{\Sigma}{360\,{\rm M}_\odot\ {\rm pc}^{-2}} \qquad (1)$$

where σ, Σ and h denote the velocity dispersion, the surface density and the depth of the LMC [2]. Reasonable values for these parameters (Gould, 1995) yield $N_{\rm LMC} \sim 1$, which is consistent with the analysis of the binary event in the recent MACHO results (Bennett et al., 1997).

The only remaining (though hardly satisfying) solution to explain the observed events toward the LMC is massive stellar remnants, white dwarfs (WD) or neutron stars (NS), as first suggested by the MACHO collaboration. Halo NS could be disk NS whose high-proper motion exceeds the disk escape velocity. However, the total number of NS in the Galatic disk amounts to $\sim 10^9$, with a NS mass strongly peaked around $\sim 1.4\,{\rm M}_\odot$. This yields a negligible ($<< 1\%$) contribution to the observed optical depth. Moreover, NS are the end product of type II supernovae, whose expected number in the Galactic halo is severely constrained by the observed metallicity. In any case NS's and stellar black holes are likely to contribute considerably less than WDs to the dark mass fraction. If the ratio of WDs to low-mass stars in the halo is assumed to be the same as the one observed in the disk, i.e. $\sim 1/100$ ($N_{WD_{disk}} \sim 3 \times 10^{-3}\,{\rm pc}^{-3}$, Liebert, Dahn & Monet, 1988) and if we assume the same amount of mass in NS - a very upper limit -, we get a *maximum contribution* of baryonic stellar remnants to the Galactic dynamic mass of $\sim$ 5%. This corresponds to less than 1 event towards the LMC. Clearly, for WDs to be responsible for the dark events towards the LMC, one must advocate very particular conditions in the primordial halo.

Recently, Chabrier, Segretain & Méra (1996) and Adams & Laughlin (1996) have examined in detail the possibility for WDs to provide a significant halo population. These authors have shown that it is indeed possible for these objects to be responsible for the observed MACHO events, thus providing $\sim$ 40% of the missing mass, under two *necessary conditions*, namely i) a halo age substantially older than the disk and a *very peculiar* halo initial mass function (IMF) strongly peaked (or cut) around $\sim 1.5 - 2\,{\rm M}_\odot$, completely different from the one determined in globular clusters and in the spheroid (Chabrier & Méra, 1997a) or in the Galactic disk (Méra, Chabrier & Baraffe, 1996; Méra et al., 1997, Paper I). This scenario also implies that a substantial fraction of the helium produced in the WD progenitors has been blown away from the Galaxy along its evolution. This is supported by the recent suggestion of the presence of hot, metal-rich gas in the Local Group (Suto et al., 1996; Fields et al., 1997), as observed in other groups of galaxies, although this scenario has been questioned recently (Gibson & Mould, 1997). Although the WD hypothesis seems very speculative and raises important questions about the nucleosynthesis of primordial intermediate-mass stars (Gibson & Mould, 1997) and requires unambigous confirmation of microlensing experiments in the Galactic halo, it cannot be excluded a priori. As shown by Chabrier et al. (1996), it is consistent with constraints arising from the expected radiation signature of the progenitors at large redshift (Charlot & Silk, 1995) and from the observed (and unobserved !) density of high velocity white dwarfs in the solar neighborhood (Liebert et al., 1988). Calculations of the expected discovery functions and star counts at faint magnitudes for various halo white dwarf luminosity functions are under way (Chabrier and Méra, 1997b), that will be confronted to

[1] It has been suggested by Gould et al. (1997) that one of these events might be due to a *disk* M-dwarf.

[2] Note that these variables are not independent from each other.

near-future high-proper-motion surveys. This will soon confirm or rule out the hypothesis of a significant halo WD population.

Interestingly enough, the WD scenario also bears important consequences on our understanding of the formation of Type Ia supernovae. If SNI form from accreting WDs, a high-density WD halo would imply 100 times more supernovae in the halo, with $M_{WD} \approx 0.40 \times 10^{12}\,\mathrm{M}_\odot$ within 50 kpc, than in the disk, where $M_{WD} \approx 0.2 \times 10^{10}\,\mathrm{M}_\odot$. Such a high rate of SNI in the halo of our Galaxy and neighbor galaxies is clearly excluded by the observations. In case WD's do indeed represent a significant halo population, this may imply that SNIa do not form from accreting WDs, as suggested by several authors (Benz et al. 1990; Mochkovitch & Livio, 1989, 1990; Nomoto & Iben, 1985; Saio & Nomoto, 1985). The final outcome of merging WDs might rather be a single, massive white dwarf (Benz et al. 1990; Segretain, Chabrier & Mochkovitch, 1997). Another possibility, in case direct observations confirm the WD hypothesis, could be that their mass function is sufficiently narrow to prevent any instability due to accretion, or that they are old enough so that mass exchanges in binary systems no longer occur.

Although other possibilities may be considered for the microlensing objects, such as, for instance, new (unknown) variable stars, hypothetical novae eruptions (Della Valle and Livio, 1996) or primordial black holes, white dwarfs remain the least unlikely solution. The models for the Galaxy can thus be split into two types: the first one postulates that the dark halo is made of matter of unknown nature and does not necessarily require the halo WD scenario (Sect. 3), the second type considers the possibility for WD-like objects to explain all, or at least most of the halo dark matter (Sect. 5).

3. Standard massive halo model

The determination of the different contributions to the dark matter density in the solar neighborhood can be understood by the following simplified analytical approach.

For a rotation velocity independent of the galactocentric distance, the Poisson equation implies a density distribution for the dark halo, assuming it is the only contributor to the dynamics:

$$\rho_h(r) = \frac{v_{\rm rot}^2}{4\pi G}\frac{1}{r^2} \tag{2}$$

where $v_{\rm rot} \approx 220$ km.s^{-1} is the asymptotic rotation velocity (see Paper I). The *maximal halo* solar density corresponds to:

$$\rho_{h\odot}^{(max)} = \frac{v_{\rm rot}^2}{4\pi G}\frac{1}{R_\odot^2} \approx 0.012\,\mathrm{M}_\odot\,\mathrm{pc}^{-3} \tag{3}$$

where $R_\odot = 8.5$ kpc is the galactocentric position of the Sun. The disk, however, contributes to the rotation velocity in the solar neighbourhood $v_\odot$. This implies a slightly reduced local halo density as compared to the maximal halo (3). At large distances, the disk exponential density-profile yields a much smaller correction. Since there is no hint for a significant drop in the observed rotation curve up to at least 70 kpc, this compensation is usually taken into account by introducing a screened halo density-profile:

$$\rho_h(r) = \frac{v_{\rm rot}^2}{4\pi G}\frac{1}{R_c^2 + r^2} \tag{4}$$

which reduces the halo density in the solar neighborhood to (for $R_c = 5$ kpc):

$$\rho_{h\odot}^{(max)} = \frac{v_{\rm rot}^2}{4\pi G}\frac{1}{R_c^2 + R_\odot^2} = 9.2 \times 10^{-3}\mathrm{M}_\odot\,\mathrm{pc}^{-3} \tag{5}$$

The rotation velocity $v_\odot$ is thus related to the halo local volume density $\rho_{h_\odot}$ and to the disk $\propto \exp(-r/R_d)$ (where R_d is the disk scale length) local surface density $\Sigma_\odot$, approximately by (see e.g. Binney & Tremaine, 1987):

$$\frac{v_\odot^2}{2\pi G} = 2f(R_c/R_\odot)R_\odot^2\rho_{h_\odot} + \frac{v_{\rm disk}^2}{2\pi G} + \frac{M_{\rm bulge}}{2\pi R_\odot} \tag{6}$$

where

$$f(x) = [1 - x\,\mathrm{Arctan}(1/x)][1 + x^2]$$
$$\tfrac{v_{\rm disk}^2}{2\pi G} = 2R_d y^2\,[I_0(y)K_0(y) - I_1(y)K_1(y)]\,\Sigma_\odot e^{R_\odot/R_d}$$
$$y = R_\odot/2R_d,$$

I_n and K_n are Bessel functions, and $M_{\rm bulge}$ is the mass of the central bulge.

On the other hand, the contributions of the disk and the halo to the vertical acceleration are given schematically by (assuming z to be small enough for $A^2 - B^2 \approx 0$, where A and B are the Oort constants):

$$\frac{K(z)}{2\pi G} = \frac{1}{2\pi G}\frac{\partial\phi}{\partial z} \approx \Sigma_\odot + 2z\rho_{h_\odot} \tag{7}$$

The standard halo model corresponds to the self-consistent solution of equations (6) and (7) which determines R_c and $\Sigma_\odot$ from the measured $v_{\rm rot}$ and $\frac{K(z)}{2\pi G}$. For $v_{rot} = 220$ km.s^{-1}, $\frac{K(z)}{2\pi G} = 71\,\mathrm{M}_\odot\,\mathrm{pc}^{-2}$ at $z = 1.1$ kpc, $R_\odot = 8.5$ kpc and $R_d = 3.5$ kpc, we get $R_c = 4.1$ kpc and $\Sigma_\odot = 49\,\mathrm{M}_\odot\,\mathrm{pc}^{-2}$, as Kuijken and Gilmore (1991). The exact determination of the respective contributions to the gravitational acceleration (7) due to the disk and halo is in fact more complicated and requires detailed (model-dependent) numerical computations (see e.g. Bienaymé, Robin & Crézé, 1987), but the present approach yields reasonnably accurate values for the dynamical constraints to be fulfilled by different disk/halo models. It is clear that *all* the values of the disk surface density derived from the measurement of the vertical acceleration in the literature were done within the standard halo model, and thus include implicitly this assumption. Any Galactic mass-model using a different (non maximal) halo will thus imply values for the observed surface density larger than the ones currently given in the litterature (since the halo contribution will be smaller than the present standard one). This important issue will be examined in Sects. 4 and 5.

We argued in Paper I that the most recent determination of the surface density by Flynn and Fuchs (1994), $\Sigma_\odot = 52 \pm 13\,\mathrm{M}_\odot\,\mathrm{pc}^{-2}$, which we use in the present calculations, is consistent at the 1σ level with all previous determinations and is nearly identical to the uncertainty-weighted average $\Sigma_\odot = 51 \pm 6\,\mathrm{M}_\odot\,\mathrm{pc}^{-2}$ of these different but consistent measurements. The density under the form of *observed* objects, determined in Paper I (Eq. 15), $\Sigma_\odot = 43 \pm 5\,\mathrm{M}_\odot\,\mathrm{pc}^{-2}$, is compatible at the 1σ level with the afore-mentioned dynamical determination, leaving limited possibility for a brown dwarf component $\Sigma_{\mathrm{BD}} = 9 \pm 14\,\mathrm{M}_\odot\,\mathrm{pc}^{-2}$. If, however, the 1σ upper limit is retained, then the disk may contain a brown dwarf density as high as $\Sigma_{\mathrm{BD}_\odot} \simeq 22\,\mathrm{M}_\odot\,\mathrm{pc}^{-2}$, *comparable to the main sequence star contribution*, still compatible with the microlensing observations towards the bulge, as shown in section 4.1.2 of Paper I.

The final parameters for the mass distribution in the Galaxy in the conventional model are thus:

• an exponential disk with a scale length $R_d = 3.5$ kpc, the surface density and brown dwarf contributions mentioned above, and a mass $M_d = 2\pi\Sigma_\odot R_d^2 \exp(R_\odot/R_d) \approx 4.6 \times 10^{10}$ $\mathrm{M}_\odot$,

• a central bar (bulge), whose maximum mass is determined below, which contributes to the microlensing optical depth with Eq. (25) of Paper I,

• a spheroid with a (flattened) De Vaucouleurs profile and a mass density deduced from the mass function given by Eq. (16) of Paper I. This yields a mass $M_{\mathrm{sph}} = 1.3 \times 10^{10}\,\mathrm{M}_\odot$, which contributes $\sim 1\%$ of the local dark matter density and $\sim 0.1\%$ of the disk total density (Chabrier & Méra, 1997a), and an optical depth $\tau_{\mathrm{sph}} \sim 5 \times 10^{-9}$ towards the LMC.

• a screened standard halo described by Eq. (4), which corresponds to a halo mass (see Sect. 2 of Paper I) $M_h = v_{\mathrm{rot}}^2 r/G \approx 10^{12}(r/100\,\mathrm{kpc})\,\mathrm{M}_\odot$. As shown in Paper I (see also Chabrier & Méra, 1997a) the contribution of main sequence stars and brown dwarfs to the halo mass budget is negligible, if not zero.

In this model, one has to invoke a substantial amount of dark matter of unknown origin.

This model gives the rotation curve shown in figure 1. We see immediately that the contribution of the central bar to the velocity at 1 kpc from the Galactic centre cannot exceed the observed value of 230 $\mathrm{km.s}^{-1}$. This sets the mass $M_{\mathrm{bulge}} \sim 1.2 \times 10^{10}\,\mathrm{M}_\odot$ within 1 kpc, under the assumption of spherical symmetry. The presence of a central bar changes this result to $M_{\mathrm{bulge}} \sim 2 \times 10^{10}\,\mathrm{M}_\odot$ (Zhao et al., 1995).

In summary, the standard halo model is consistent with all observed properties of the Galaxy, at the price of postulating the existence of a sizeable fraction of non-baryonic matter in the halo (that is needed anyway at larger scales if the density parameter of the Universe Ω is larger than 0.1). To explain the observed microlensing events towards the LMC, the only (uncomfortable) possibility is to invoke a substantial amount of white dwarfs in the halo, which contribute to $\sim 40\%$ of the dynamical mass, providing very particular hypothesis on the age and the initial mass function of the halo, as discussed in the previous section. Since, as mentioned above, brown dwarfs and low-mass stars seem to be excluded as a significant halo population, this model implies that $\sim 60\%$ of the Galactic missing mass is in the form of undetected *non-baryonic* matter. This fraction may be as high as 90% if the lower limit for the baryonic fraction in the halo inferred from the number of microlensing events is retained. Note, however, that this model does not *need* a white dwarf component in the halo. Would the future number of microlensing events towards the LMC decrease, or even vanish, this model remains valid.

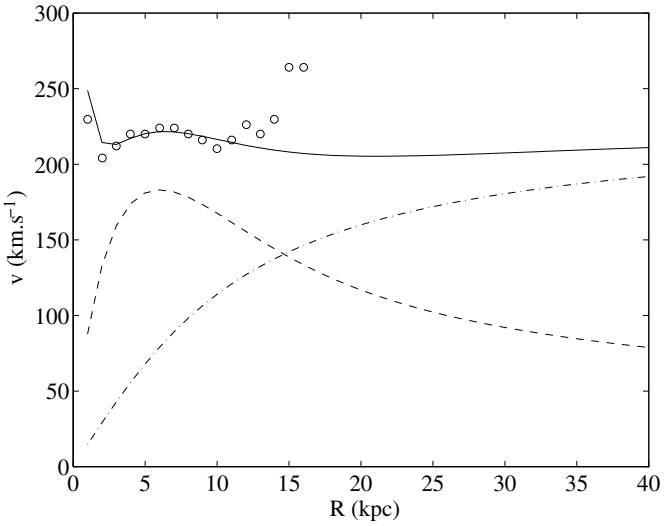

Fig. 1. Rotation curve of the standard model (see text). The open circles correspond to the averaged observed values (from Vallée, 1994), the dashed line is the disk contribution, the dash-doted line the halo contribution, and the solid line is the total model rotation curve.

4. Maximal disk

It has been proposed recently on various grounds (e.g. Pfenniger, Combes & Martinet, 1994) that, contrary to the original suggestion of Ostriker and Peebles (1973), the Galaxy has no massive dark halo. In this case, *all* dark matter is distributed in a strongly flattened, disk-like structure.

It is well known that an exponential disk gives rise to a decreasing rotation curve, incompatible with the observed flat rotation curve (see e.g. Binney & Tremaine, 1987). The inverse problem, which consists of deriving a density profile from an observed rotation curve, can be solved analytically for the peculiar case of a constant rotation velocity (Mestel, 1963). For an *infinite* disk, the surface density is proportional to the radial distance $1/R$:

$$\Sigma(R) = \Sigma_\odot \frac{R_\odot}{R} \tag{8}$$

with

$$\Sigma_\odot = 208\,(\frac{v_{\mathrm{rot}}}{220\,\mathrm{km.s}^{-1}})^2\ \mathrm{M}_\odot\,\mathrm{pc}^{-2} \tag{9}$$

This value is much larger than the one inferred from the observed vertical acceleration (see Paper I).

As mentioned above, Eq. (8) holds for an *infinite* disk. The *finite-size* yields a smaller value for $\Sigma_\odot$ for the same rotation curve. In this case, the density profile is very close to an exponential, $\Sigma(R) \approx \Sigma_0 e^{-R/R_d}$, with a scale length $R_d \approx 1/3\, R_G$, where R_G is the Galactic (disk) radius (Méra, Mizony & Baillon, 1997). Only the very central and external parts of such a maximal disk depart from the exponential profile, as expected. In the centre, this departure corresponds to the bulge whereas at the edge, the density must decrease to zero. Thus, for a *truncated disk*, a flat rotation curve does not correspond to a $1/R$ surface density but rather to an *exponential* disk profile plus a central bulge (see Méra, Mizony & Baillon, 1997). The scale length of this exponential is $R_d \sim 10$ kpc for spiral galaxies similar to the Milky Way, which corresponds to an exponential variation of the mass-to-light ratio M/L in the Galactic disk, and an increasing dark matter/visible matter ratio from the centre to the edge of the disk. As demonstrated by Méra et al. (1997b), if all the mass is distributed in a disk, the local surface density is fixed essentially by the disk radius R_G. For the rotation curve to be flat up to at least R_G = 30 kpc, we get:

$$\Sigma_\odot \geq 190\, \mathrm{M}_\odot\, \mathrm{pc}^{-2} \tag{10}$$

As stressed in Sect. 2, the "observed" dynamical densities are derived by measuring $K(z)$ at some altitude z, corrected from the standard halo contribution to obtain the disk density. If the halo local density is reduced, the disk surface density implied by a given vertical acceleration is different (Eq. (7)). For the standard halo (Sect. 3), the halo correction yields:

$$\Sigma_\odot = \frac{K(\langle z \rangle)}{2\pi G} - 20\, \mathrm{M}_\odot\, \mathrm{pc}^{-2} \frac{\langle z \rangle}{1\ \mathrm{kpc}} \tag{11}$$

where $\langle z \rangle$ is the average height of the sample.

In case there is no halo (maximal disk), $20\, \mathrm{M}_\odot\, \mathrm{pc}^{-2} \frac{\langle z \rangle}{1\ \mathrm{kpc}}$ must be added to the $\Sigma_\odot$ values quoted by the various authors. With our estimate of $\langle z \rangle$ = 1 kpc, 1.1 kpc, 0.5 kpc and 0.5 kpc for the Bienaymé et al (1987), Kuijken and Guilmore (1991), Bahcall et al (1992) and Flynn and Fuchs (1994) surveys, respectively, the observed values become $\Sigma_\odot = 70 \pm 10, 70 \pm 9, 95 \pm 25, 62 \pm 13\, \mathrm{M}_\odot\, \mathrm{pc}^{-2}$, respectively, with an average $70 \pm 6\, \mathrm{M}_\odot\, \mathrm{pc}^{-2}$ [3]. Therefore, the surface density (10) needed to comply with the rotation curve is many standard deviations off the observed value.

One may argue that the vertical distribution of the gas increases with Galactocentric distances, as expected if the gas is supported by rotation (Pfenniger et al, 1994). This would yield a dark "corona" beyond the edge of the observed optical disk. However, this is not a satisfactory solution, since, as can be shown easily, adding a dark corona of matter *outside* the disk will *lower* the rotation velocity inside the Galactocentric radius of this corona, so that the disk surface density must be increased accordingly in order to reproduce the observed rotation velocity, to a value close to (9).

In sum, the total mass of the disk in this model is $M_d \approx 10^{11} \times R_G/10$ kpc. It seems unrealistic that the disk extends beyond 40 kpc for stability reasons so that such a description of our Galaxy would not be consistent with the velocity fields observed up to 60 kpc (see Sect. 2 of Paper I). It similarly implies that the mass of the Milky Way is significantly smaller than the required $2.4 \pm 0.8 \times 10^{12}\, \mathrm{M}_\odot$ deduced from the dynamics of the Local Group (Peebles, 1994; see Sect. 2 of Paper I). Or it would impose that almost all the mass of the Local Group ($\sim 4 \times 10^{12}$ $\mathrm{M}_\odot$) is in Andromeda. The dynamics of our Galaxy would be explained without the presence of non-baryonic dark matter at the price of an unacceptably large amount of such material in Andromeda.

The only way out is to require *the dark matter to be distributed over a scale height $z > 3$ kpc*. In this case, the maximal disk is similar to a highly flattened halo, a solution apparently not supported by observations, as mentioned in Sect. 2. If the sought baryonic matter is in the form of dark, molecular hydrogen clouds (Pfenniger et al, 1994; Gerhard & Silk, 1996), this raises a severe problem, for the observed distribution of *atomic* hydrogen (Dickey and Lockman, 1990) is well confined within 200 pc from the Galactic plane. This implies that molecular and atomic hydrogen gas must have a completely different (a factor 10) Galactic scale height.

In summary, the maximal disk or highly flattened halo models seem to be excluded by kinematic observations and a 3-dimensional dark halo contribution is necessary, which is responsible for the constant (non-keplerian) rotation curve beyond the disk truncation radius.

5. Modified halo model

As shown in Eq. (4), the halo distribution is determined by two parameters: its size, fixed by the total Galactic mass, and its core radius R_c. This latter is not physically motivated but is determined by the condition that the visible plus dark matter distributions give rise to the measured rotation curve, which yields the local halo normalization. The standard halo model (Sect. 3) assumes by definition that the dark matter is mostly in the dark halo, so that the local halo density is $\rho_{h_\odot} = 9 \times 10^{-3}\, \mathrm{M}_\odot\, \mathrm{pc}^{-3}$ and $R_c = 5 \pm 1$ kpc (Eq. 5).

We modify the standard model by putting as much baryonic mass in the disk as allowed by the microlensing observations and the star counts, from the analysis conducted in Paper I. The aim is to derive the maximum limit of a predominantly baryonic model for the Galaxy compatible with all presently available observations.

We first note that there is observational evidence that the optical disk is truncated at a galactocentric distance $R \approx 14$ kpc (Robin, Crézé & Mohan, 1992; Ruphy et al., 1996). As mentioned in section Sect. 4, such a truncated disk plus a central bulge yield a flat rotation curve up to the limit of the disk, with a scale length $R_d \approx 3.3$ kpc, in agreement with observations

[3] As mentioned in Paper I, the Bahcall et al. (1992) and Flynn & Fuchs (1994) observations are not completely independent but the weight of the Bahcall et al. value is small and droping it does not affect the result.

($1.8 < R_d < 5$ kpc, see Kent, Dame & Fazio, 1991) and $\Sigma_\odot \approx 120\,\mathrm{M}_\odot\,\mathrm{pc}^{-2}$ (Méra et al., 1997b). Since a maximal disk is excluded (Sect. 4), we must include a halo contribution given by the following flattened distribution (in cylindrical coordinates):

$$\rho_h(R,z) = \rho_{h_\odot} \frac{R_\odot^2 + R_c^2}{R^2 + z^2/q^2 + R_c^2} \tag{12}$$

with

$$\rho_{h_\odot} = f \times \frac{v_{\rm rot}^2}{4\pi G} \frac{1}{R_c^2 + R_\odot^2} \frac{\sqrt{1-q^2}}{q\,\mathrm{Arccos}q}, \tag{13}$$

where f is the normalization of the halo, and $q \sim 0.6$. Straightforward calculations yield the following expression for the contribution of such a halo to the rotation curve:

$$v_h^2 = f\,v_{\rm rot}^2 \left[1 - \frac{R_c\,\epsilon}{\sqrt{R_c^2\,\epsilon^2 + R^2}} \frac{\mathrm{Arctan}\frac{1}{q}\sqrt{\epsilon^2 + R^2/R_c^2}}{\mathrm{Arcsin}\,\epsilon}\right] \tag{14}$$

where $\epsilon = \sqrt{1-q^2}$. For $R >> R_c$, the asymptotic rotation velocity is $\sqrt{f} v_{\rm rot}$, with $v_{\rm rot} \approx 220$ km.s^{-1}.

The core radius R_c plays in fact the same role as the normalization factor f, as shown by eqn. (12). Halo models (f = 0.35; R_c = 5 kpc) and (f = 1; R_c = 15 kpc) yield the same normalization in the solar neighborhood $\rho_{h_\odot} = 3\times10^{-3}\,\mathrm{M}_\odot\,\mathrm{pc}^{-3}$, i.e. $\sim$ 30% of the standard model local density, but the second one yields the *correct rotation velocity at large distances* ($R \gtrsim 20$ kpc). A truncated disk plus a dark halo with a large core-radius, $R_c \sim 15$ kpc is thus a solution worth considering. This model is consistent with the microlensing experiments towards the LMC which yield a dark matter contribution $\sim$ 40% of the standard halo: the microlensing optical depth toward the LMC derived from the afore-mentioned density is $\tau = 3\times10^{-7}$, in agreement with the observed value.

We have substracted the contribution of this modified halo from the observed rotation curve, taken from Vallée (1994), up to $\sim$ 14 kpc. Fig. 2 shows the inferred density profile for the disk. The agreement between theory and observation yields a scale length R_d = 3.2 kpc and a disk mean surface density $\Sigma_\odot = 87\,\mathrm{M}_\odot\,\mathrm{pc}^{-2}$.

Instead of using the numerical density profile derived from the inversion technique of Méra et al. (1997b), we will use the more simple exponential density law. Then the observed rotation curve is well reproduced with the following disk density:

$$\Sigma_d(R) = (75\ \mathrm{M}_\odot\,\mathrm{pc}^{-2})\ e^{R_\odot/R_d}\ e^{-R/R_d}$$

Fig. 3 shows the total (disk + halo) rotation curve up to 60 kpc. The disk dominates the rotation curve up to its edge, i.e. $\sim$ 14 kpc, whereas the dark halo becomes dominant beyond this limit and reaches the correct asymptotic value 220 km.s^{-1}. The rotation curve of the model departs significantly from the observations for $R > 12$ kpc, but the uncertainty begins to be large at these radii (about 20%). In particular, the last two points are derived from 5 objects only, each with large errors. Therefore, we can consider the model as consistent with the observed rotation curve.

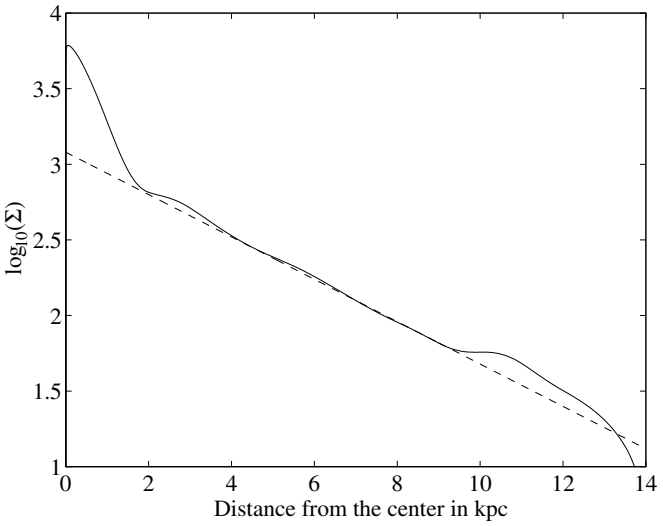

Fig. 2. Surface density profile of the Galactic disk inferred from the observed rotation curve (Vallée, 1994), from which the modified-halo (R_c = 15 kpc) contribution has been removed (see text). The dashed line is an exponential profile of scale length 3.2 kpc, and solar density 87 $\mathrm{M}_\odot\,\mathrm{pc}^{-2}$.

The most interesting property of this model is that it is consistent with a *fully baryonic* dark matter solution, most of the matter being in the dark halo, and some of it in the disk. The disk dark population consists of brown dwarfs (see Sect. 4.1.2 of Paper I), whereas for the halo, the most likely candidates are white dwarfs, as discussed in Sect. 2. As discussed at length in Sect. 3.1 and §4.1 of Paper I, a substantial population of disk brown dwarfs is consistent with present-day microlensing observations toward the Galactic center. It is also consistent with the extrapolation into the sub-stellar domain of the M-dwarf mass function obtained either from the nearby luminosity function (Kroupa, 1995) or from the very faint end of the HST luminosity function (Gould et al., 1997), if the apparent upturn in this region is real. Such mass functions $dN/dm \propto m^{-\alpha}$ have a slope $\alpha \gtrsim 2$ and a normalization near the bottom of the main sequence $dN/dm(0.1\,\mathrm{M}_\odot) \sim 1\,\mathrm{M}_\odot^{-1} pc^{-3}$ (see Sect. 3.1 of Paper I).

A rising MF near the brown dwarf domain is supported by the recent study of the distribution of secondary masses of 20 F and G dwarf binaries by Mazeh, Latham & Stefanik (1996), although poor statistics (3 detections) preclude the derivation of a precise MF. On the other hand, a shallower MF or a substantially smaller normalization near the bottom of the MS will rule out the possibility of a substantial brown dwarf mass-fraction in the Galactic disk. Therefore nailing down the issue on the very end of the disk MF bears essential consequences for Galactic modelling. This should be done shortly with the DENIS whole-sky survey.

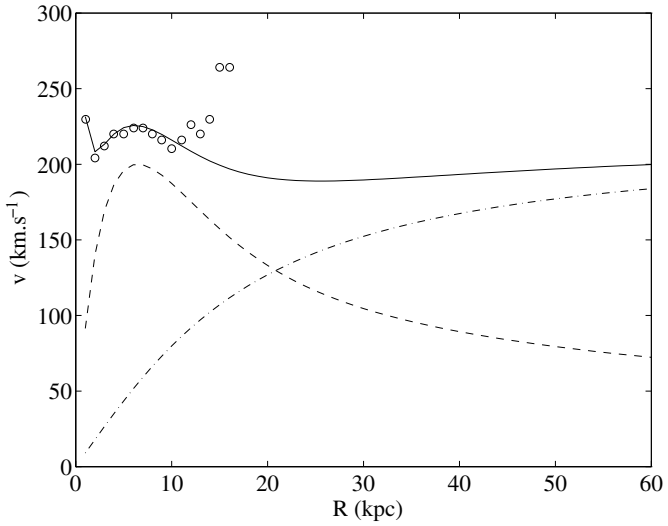

Fig. 3. Rotation curve of the modified halo model. The disk contribution corresponds to the dashed line, while the halo contribution corresponds to the dash-dotted line. The solid line is the total rotation curve, with the observed rotation curve (Vallée, 1994) for $R < 14$ kpc. Note that the observational uncertainties become very large beyond 10 kpc (see Fich & Tremaine, 1991).

As shown above, the main problem of such a modified-halo model is the large inferred surface density $\Sigma_\odot \sim 75\,\mathrm{M}_\odot\,\mathrm{pc}^{-2}$. For this model, the halo correction is only

$$\Sigma_\odot \;=\; \frac{K(\langle z\rangle)}{2\pi G} \;-\; 6\,\mathrm{M}_\odot\,\mathrm{pc}^{-2}\frac{\langle z\rangle}{1\,\mathrm{kpc}}, \qquad (15)$$

so we have to increase by 14 (20 minus 6) $\mathrm{M}_\odot\,\mathrm{pc}^{-2}\frac{\langle z\rangle}{1\,\mathrm{kpc}}$ the observed dynamical values. This yields $\Sigma_\odot = 63 \pm 10,\ 62 \pm 9,\ 91 \pm 25,\ 58 \pm 13\ \mathrm{M}_\odot\,\mathrm{pc}^{-2}$ for Bienaymé et al (1987), Kuijken and Gilmore (1989), Bahcall et al (1992), Flynn and Fuchs (1994) determinations, respectively, with the average $\Sigma_\odot = 63 \pm 6\,\mathrm{M}_\odot\,\mathrm{pc}^{-2}$. Since the detected surface density is $\Sigma_{\odot_{vis}} = 43 \pm 5\,\mathrm{M}_\odot\,\mathrm{pc}^{-2}$ (Eq. 15 of Paper I), the brown dwarf surface density in the solar neighborhood is then $\Sigma_{\mathrm{bd}} = 15 \pm 14$, still compatible with microlensing observations (see Sect. 4.1.2 of Paper I).

The axisymmetric mean density at the solar radius $\Sigma_\odot \approx 75\,\mathrm{M}_\odot\,\mathrm{pc}^{-2}$ obtained in this model is larger by ~ 1.3 standard deviations than the afore-mentioned Flynn & Fuchs (1994) recent determination in the solar neighborhood. The difference, however, may be attributed to the fact that the Sun is located in-between two spiral arms, namely ~ 1.5 kpc from the Sagittarius arm and ~ 2 kpc from the Perseus arm (King, 1989). Therefore the solar surface density might be slightly smaller than the averaged surface density along the circle of radius $R_\odot$. This is supported by the observations of external galaxies and by numerical simulations, which give about a factor 2 for the maximal/minimal density in the disk, expected to translate into a smaller factor for the vertical acceleration $K(z)$ (see e.g. Rix and Zaritsky, 1995). The value at 1.1 kpc of $K_z/2\pi G$ derived by Kuijken and Gilmore (1991) is $71 \pm 6\,\mathrm{M}_\odot\,\mathrm{pc}^{-2}$, whereas for the present heavy disk model $K_z/2\pi G = 81\,\mathrm{M}_\odot\,\mathrm{pc}^{-2}$, corresponding to a ratio of 1.14, which could be acco unted for by the spiral structure.

The average density we need is ~ 1.3 times larger than the mean solar value, and only 5% times larger than the 1-σ upper limit of the Flynn and Fuchs (1994) value. Although the relevance of such values deserves a detailed study, they do not seem to be unrealistic.

6. Summary and conclusions

In the present paper, we have derived consistent mass-models for the Galaxy, disk(s), bulge, spheroid and dark halo. The present calculations differ substantially from previous approaches which relied on microlensing analysis only (e.g. Alcock et al., 1996b) or which were based on the minimization of models with a large number of free parameters (e.g. Gates, Gyuk and Turner, 1996). We proceed differently by first determining as accurately as possible the main parameters entering the Galactic modelling from *all* observational constraints presently available, i.e. star counts and luminosity functions of metal-rich and metal-poor M-dwarfs at faint magnitudes, including the most recent Hubble Deep Field data, microlensing observations towards the LMC and the central part of the Galaxy, including not only the optical depths but the much more constraining time-distributions of the events, and large-scale (circular rotation velocity) and small-scale (local gravitational acceleration) kinematic properties. The microlensing analysis is derived not only in term of optical depth but includes the complete time-distributions of the events. These calculations include previous results wich yield the determination of the mass-functions in the Galactic disk (Méra, Chabrier & Baraffe, 1996) and spheroid (Méra, Chabrier & Schaeffer, 1996; Chabrier & Méra, 1997a) and of the contribution of stellar and substellar objects to the Galactic disk and halo mass budgets (Méra, Chabrier & Schaeffer, 1997; Paper I; Chabrier & Méra, 1997a). This yields a *consistent* determination of the different parameters.

We show that a maximal disk model is clearly excluded by the observations, in particular by the observed local surface density. An extension of this model, where dark matter is in the form of giant molecular clouds located at the very periphery of the Galactic disk (Pfenniger et al, 1994) raises severe problems: i) it implies that molecular hydrogen is distributed over a scale *height* about 10 times larger than the observed *atomic* hydrogen distribution, for the surface density to agree with the observed value, ii) it implies a scale *length* for the disk $R_d \sim 10$ kpc, about 3 times larger than the value deduced from star counts, for the circular rotation velocity to be constant up to ~ 30 kpc, iii) it does not explain the observed microlensing events toward the LMC. In case such clouds are distributed in the halo (Gerhard & Silk, 1996), point i) and iii) remain valid. An extension of this model, namely a highly flattened ($q \sim 0.1$) halo, although not completely ruled out, is at odd with various observational constraints (see Sect. 2).

Two models (and possibly a whole range of models in-between these extremes) fulfill *all* the afore-mentioned observational contraints. The various components of these two models are given in Table 1. Both include:

• a central, elongated bulge, with $M_{\rm bulge} \sim 2 \times 10^{10}\,{\rm M}_\odot$ from kinematic considerations. The analysis of the first year of MACHO observations towards the bulge (Alcock et al., 1997) seems to exclude a significant population of brown dwarfs in this region (Paper I) although better statistics are needed to really nail down this issue,

• a thin double-exponential disk with a scale length $R_1 \sim 3$ kpc and a scale height $h_1 \sim 320$ pc (Bahcall & Soneira, 1980) (or equivalently a sech^2 × exp model (Gould et al., 1997)), + a thick sech^2 ($|z|/h_2$) disk with the same scale length, a scale height $h_2 \sim 640$ kpc and a local normalization $\sim 20\%$ (Gould et al., 1997). The mass of the disk reads:

$$M_{\rm disk} \approx 2\pi\Sigma_\odot R_d^2 e^{R_\odot/R_d} \tag{16}$$

where $\Sigma_\odot$ is the local mass density, which is different in the two models.

• a flattened ($q \sim 0.6$) DeVaucouleurs spheroid with a mass $M_{\rm sph} \approx 1.3 \times 10^{10}\,{\rm M}_\odot$, i.e. a negligible contribution to the Galactic mass budget (Chabrier & Méra, 1997a),

• a flattened dark halo with the density profile (12), which yields a mass:

$$\begin{aligned} M_h &= \frac{v_{\rm rot}^2}{G}(R_h - R_c\,{\rm Arctan}\frac{R_h}{R_c}) \\ &\approx 1.36 \times 10^{12}\,\frac{R_h + 23\,{\rm kpc}}{100 + 23\,{\rm kpc}}\,{\rm M}_\odot, \end{aligned} \tag{17}$$

which is nearly independent of the value of the core radius R_c.

In both models, a significant contribution of low-mass stars and brown dwarfs to the dark halo mass is excluded from star count observations and microlensing experiments (Chabrier & Méra, 1997a; Méra, Chabrier & Schaeffer, 1997). Although we can argue that neither the EROS nor the MACHO experiments are optimized for short-duration ($\sim$ days) observations[4], a significant population of low-mass (brown dwarfs) objects in the halo would produce *many* short-time events: $N = \Gamma \times E \times \epsilon$, where $E = 1.8 \times 10^7$ star.year is the exposure of the MACHO collaboration, ϵ is their mean detection efficiency and $\Gamma \sim 1.6 \times 10^{-6}\,(m/{\rm M}_\odot)^{-1/2}$ event/year is the event rate for the standard halo model. A Dirac MF in the BD domain $m \lesssim 0.1{\rm M}_\odot$ implies about 16 events with $t_e \lesssim 20$ days, which is excluded at 99% confidence level, since only one has been observed (with $t_e \approx 19.4$ days, Alcock et al., 1996b). Planetary-like objects ($m < 10^{-2}\,{\rm M}_\odot$) are also excluded as a significant mass-contribution ($\gtrsim 10\%$) at 95% confidence level by the EROS CCD observations (Renault et al., 1997) and the MACHO "spike" observations (Alcock et al., 1996a). In both models also, the dark halo contains a significant population of compact objects, which are responsible for the microlensing observations towards the LMC and amount to a local density $\rho \sim 3 \times 10^{-3}\,{\rm M}_\odot\,{\rm pc}^{-3}$. As mentioned below, this condition is *compulsory* for the second (modified halo) model. Although uncomfortable, the halo WD solution represents the "least unlikely" scenario and cannot be excluded at the time these lines are written.

[4] Although the EROS CCD experiment was optimized for short timescales, the exposure, $\sim$ 80000 stars × a few months, is small.

Table 1. Main characteristic of the two consistent Galactic models outlined in the Conclusion. The dark halo is made of white dwarfs in both models, but the standard model has a dominant non baryonic component.

	Std halo	heavy disk	unit
Disk:			
Scale length	3.2	3.2	kpc
Scale height	320	320	pc
$\rho_{\rm bd}$	$\lesssim 0.015$	~ 0.03	${\rm M}_\odot\,{\rm pc}^{-3}$
Mass	3×10^{10}	5×10^{10}	${\rm M}_\odot$
Thick Disk:			
Scale length	3.2	3.2	kpc
Scale height	640	640	pc
Mass	6×10^9	6×10^9	${\rm M}_\odot$
Bulge:			
Mass	1.2×10^{10}	1.2×10^{10}	${\rm M}_\odot$
Bar	yes	yes	
Brown dwarfs	none	none	
Spheroid:			
Density	De Vaucouleurs	De Vaucouleurs	
Oblateness	$q \sim 0.6$	$q \sim 0.6$	
Mass	1.3×10^{10}	1.3×10^{10}	${\rm M}_\odot$
Halo:			
Core radius	5	14	kpc
Composition	$< 50\%$ WD	up to 100% WD	
Mass	$\sim 10^{12}$	$\sim 10^{12}$	${\rm M}_\odot$
v_∞	220	220	${\rm km.s}^{-1}$
Total column density:			
$\langle\Sigma\rangle$ at $R_\odot$	~ 55	~ 75	${\rm M}_\odot\,{\rm pc}^{-2}$

The very difference between these two models resides in the location of the Galactic dark matter. The first model is simply what we call the "standard" model with a *possible* ($\sim 10 \pm 10\,{\rm M}_\odot\,{\rm pc}^{-2}$) amount of hidden mass under the form of brown dwarfs in the disk or in the bulge. In this case, *nearly all* dark matter is in the dark halo and is predominantly ($> 50\%$) of *non-baryonic nature*. In the second case, the Galactic disk must necessarily include a significant brown dwarf population. The analysis conducted in Paper I (Sect. 4.1.2) yields a brown dwarf contribution $\Sigma_{\odot_{\rm BD}} \sim 20 - 30{\rm M}_\odot\,{\rm pc}^{-2}$, comparable to the stellar contribution, and thus a local surface density $\Sigma_\odot \simeq 60 - 70\,{\rm M}_\odot\,{\rm pc}^{-2}$, since $\Sigma_{\odot_{\rm vis}} = 43 \pm 5\,{\rm M}_\odot\,{\rm pc}^{-2}$ (Eq. (15) of Paper I), within the 1σ limits of the observed dynamical value (Flynn & Fuchs, 1994). The *average* disk surface density at the solar radius is in this model $\sim 5 - 20\%$ larger than the dynamical value determined in the solar neighborhood. This may be due to the presence of density waves. Most of the dark matter is still in the dark halo but its contribution to the local dynamical density amounts only to $\sim 3 \times 10^{-3}\,{\rm M}_\odot\,{\rm pc}^{-3}$,

$\sim$ 30% of the *standard* halo contribution. This (heavy disk) model necessarily needs the presence of white dwarfs (or other remnants) in the halo to be confirmed, these latter providing most of the missing mass. In this case, the missing mass in spiral galaxies is *entirely baryonic* and the dark baryons consist essentially of brown dwarfs in the disks and white dwarfs in the halos. This model, however, must be considered as an extreme case. But it shows the possibility of a heavy Galactic disk, with a substantial fraction of brown dwarfs, which yields a smaller local normalization for the halo than assumed in the usual standard disk+halo model. This leads to a *predominantly*, rather than "entirely" baryonic model, a more likely solution. This model, however, requires a rather large surface density in the solar neighborhood and a relatively steep ($\alpha \sim 2$) mass function in the disk near the hydrogen-burning limit, which extends apparently (within the present uncertainties) to smaller masses than in the bulge (see Paper I, Sect. 4.1.1 and 4.1.2).

Therefore, the key issue to determine the correct Galactic mass-model, based on the present analysis, is the determination of i) the brown dwarf density in the disk/bulge and ii) the white dwarf (or other candidates) density in the dark halo. Ongoing microlensing experiments (EROS II, MACHO), infrared surveys and large field high-proper motion surveys might soon nail down this issue. Analysis of these observations in the context of the present models will yield immediatly the contributions of the various baryonic components to the different parts of the Galaxy and eventually the characterization of the (at least baryonic) dark matter in the Galaxy. Meanwhile, the DENIS and 2MASS projects should allow a precise determination of the disk stellar mass function down to (perhaps below) the hydrogen-burning limit, allowing more robust extrapolation into the brown dwarf domain. Unfortunately, observations at the time these lines are written do not allow to disentangle between these two models. Various uncertainties in present-day observations (scale heights, scale lengths, $v_{\rm rot}, \Sigma_\odot, R_\odot$, microlensing observations) remain within the error bars allowed by the present models.

We have shown in the present paper that both types of models yield the observed, constant circular rotation curve up to large galactocentric distances. In particular a truncated disk yields an *exponential* density profile. In the second model, the disk contributes to the rotation curve up to its edge, and the dark halo beyond this limit. Both the disk and the halo yield a flat rotation curve and there is *no need anymore to invoke any peculiar conspiracy*. We stress that, in virtue of the Occam's razor principle, we have considered in the present calculations the most natural hypothesis for the nature and the location of dark matter. We have assumed in particular that the dark matter is distributed homogeneously, as visible matter. This yields about constant, but different, mass-to-light ratios in the disk and in the halo. We have not considered more exotic scenarios involving clustered dark matter in the halo (see e.g. Kerins, 1997). We believe the present calculations to provide new insight on the possible nature and distribution of dark matter in galaxies. Comparisons of future observations with the present models should help answering this long-standing problem.

Acknowledgements. We have benefited all along this work of numerous discussions with various people, more particularly with the MACHO and the EROS groups and with D. Pfenniger and F. Combes. We also acknowledge useful conversations with O. Gerhard and with the referee, A. Gould. It is a pleasure to thank these persons for their valuable help.

References

Adams, F. and Laughlin, G., 1996, ApJ 468, 586
Alcock, C. et al., 1996a, ApJ 471, 774
Alcock, C. et al., 1996b, ApJ 461, 84
Alcock, C. et al., 1997, ApJ 479, 119
Bahcall, J., Flynn, C., and Gould, A., Kirhakos, S., 1994, ApJ 435, L51
Bahcall, J., Flynn, C., and Gould, A., 1992, ApJ 389, 234
Bahcall, J. and Soneira, R., 1980, ApJS 44, 73
Bennett, D. et al., 1997, Submitted to Nuclear Physics B
Benz, W., Cameron, A., Press, W., and Bowers, R., 1990, ApJ 348, 647
Bienaymé, O., Robin, A., and Crézé, M., 1987, A&A 180, 94
Binney, J. and Tremaine, S., 1987, Galactic dynamics, Princeton University Press
Bissantz, N., Englmaier, P., Binney, J., and Gerhard, O., 1996 MNRAS, submitted
Carr, 1994, ARA&A, 32, 531
Chabrier, G. and Méra, D., 1997a, A&A 328, 83
Chabrier, G. and Méra, D., 1997b, in preparation
Chabrier, G., Segretain, L., and Méra, D., 1996, ApJ 468, L21
Charlot, S., and Silk, J, 1995 ApJ 445, 124
Copi, C., Schramm, D., and Turner, M., 1995, Science 267, 192
Dahn, C., Liebert, J., Harris, H., and Guetter, H., 1995, in C. Tinney (ed.), The bottom of the main sequence - and beyond, p. 239, ESO, Springer-Verlag, Berlin
Della Valle, M. and Livio, M., 1996, ApJ 457, L77
Dickey., J. and Lockman, F., 1990, ARA&A 28, 215
Evans, N.W., 1993 MNRAS 260, 191
Evans, N.W., 1994 MNRAS 267, 333
Fich, M. and Tremaine, S., 1991, ARA&A 29, 409
Fields, B., Mathews, G., and Schramm, D., 1997, ApJ 483, 625
Flynn, C. and Fuchs, B., 1994, MNRAS 270, 471
Gates, E. I., Gyuk, G., and Turner, M. S., 1996, Phys. Rev. Dl 53, 4138
Gerhard, O. & Silk, J., 1996 ApJ 472, 34
Gibson, J. and Mould, J., 1997, ApJ 482, 98
Gilmore, G., 1984, MNRAS 207, 223
Gould, A., 1995, ApJ 441, 77
Gould, A., Bahcall, J., and Flynn, C., 1997, ApJ 482, 913
Graff, D. and Freese, K., 1996, ApJ 456, L49
Kent, S., 1992, ApJ 387, 181
Kent, S., Dame, T., and Fazio, G., 1991, ApJ 378, 131
Kerins, E., 1997, A&A, in press
King, I., 1989, Saas-Fee 19, The Milky Way Galaxy, Eds. I. King, G. Gilmore and van der Kruit
Kroupa, P., 1995, ApJ 453, 358
Kuijken, K. and Gilmore, G., 1989, MNRAS 239, 605
Kuijken, K. and Gilmore, G., 1991, ApJ 367, L9
Liebert, J., Dahn, C., and Monet, D., 1988, ApJ 332, 891
Mazeh, T., Latham, D., & Stefanik, 1996 ApJ 466, 415
Méra, D., Chabrier, G., and Baraffe, I., 1996a, ApJ 459, L87

Méra, D., Chabrier, G., and Schaeffer, R., 1996b, Europhysics Letters 33(4), 327
Méra, D., Chabrier, G., and Schaeffer, R., 1997a, Submitted to Paper I A&A
Méra, D., Mizony, M., and Baillon, J., 1997b, Submitted to A&A
Mestel, L., 1963, MNRAS 126(6), 553
Mochkovitch, R. and Livio, M., 1989, A&A 209, 111
Mochkovitch, R. and Livio, M., 1990, A&A 236, 378
Nomoto, K. and Iben, I., 1985, ApJ 287, 531
Ostriker, J. and Peebles, P., 1973, ApJ 186, 467
Peebles, P., 1994, ApJ 429, 43
Pfenniger, D., Combes, F., and Martinet, L., 1994, A&A 285, 79
Renault, C. et al., 1997, preprint astro-ph/9612102, submitted to A&A
Rix , and Zaritsky, 1995 ApJ 447, 82
Robin, A., Crézé, M., and Mohan, V., 1992, ApJ 400, L25
Ruphy, S., Robin, A., Epchtein, N., Copet, E., Bertin, E., Fouqué, P., and Guglielmo, F., 1996, A&AL 313, L21
Sackett, P., Morisson, H., Harding, P., and Boroson, T., 1994, Nature 370, 441
Saio, H. and Nomoto, K., 1985, A&A 150, L21
Santiago, B.X., Gilmore, G. & Elson, R.A.W., 1996 MNRAS 281, 871
Segretain, L., Chabrier, G., and Mochkovitch, R., 1997 ApJ 481, 355
Suto, Y., Makishima, K., Ishisaki, Y., and Ogasaka, Y., 1996, ApJ 461, L33
Vallée, J., 1994 ApJ 437, 179
Zhao, H., Spergel, D., and Rich, R., 1995, ApJ 440, L13

Note added in proof: After the present calculations were completed of the local dynamical density has been derived from the Hipparcos data (Crézé et al., astro-ph/9709022). This new determination leaves essentially no room for any dark component in the disk and thus, if confirmed, seems to exclude the modified-halo model (Sect. 5) and to confirm the standard halo model (Sect. 3).

This article was processed by the author using Springer-Verlag LaTeX A&A style file *L-AA* version 3.